QUANTITATIVE STUDIES ON THE POLARIZATION OPTICAL PROPERTIES OF STRIATED MUSCLE

I. Birefringence Changes of Rabbit Psoas Muscle in the Transition from Rigor to Relaxed State

D. LANSING TAYLOR

From the Marine Biological Laboratory, Woods Hole, Massachusetts 02543 and The Biological Laboratories, Harvard University, Cambridge, Massachusetts 02138

ABSTRACT

The changes in birefringence in the rigor to relax transition of single triton-extracted rabbit psoas muscle fibers have been investigated with quantitative polarized light techniques. The total birefringence of rest length fibers in rigor was $(1.46 \pm 0.08) \times 10^{-3}$ and increased to $(1.67 \pm 0.05) \times 10^{-3}$ after Mg-ATP relaxation. Pyrophosphate relaxation increased the total birefringence only slightly, whereas subsequent Mg-ATP relaxation elicited the maximum increase in birefringence. Changes in lattice spacing did not account for the total increase in birefringence during relaxation. Moreover, the increase in total birefringence was attributable to increases in intrinsic birefringence as well as form birefringence. No change in birefringence was exhibited upon exposure to a relaxation solution after myosin extraction.

Synthetic myosin filaments were prepared and treated with relaxation and rigor solutions. The negatively stained filaments treated with a rigor solution had gross irregular projections at either end, while the filaments treated with a relaxing solution were more spindle shaped. The results are compatible with the view that the subfragment-2 moieties of myosin angle away from the myosin aggregates (light meromyosin) to permit the attachment of the subfragment-1 moieties to actin.

It is commonly accepted that the force generation mechanism in vertebrate striated muscle involves the angular movements of the subfragment-1 (S-1) moieties upon attachment to the actin filaments (16, 15, 9, 27). However, a simple mechanical interaction between the S-1 moieties and actin is not possible since the center-to-center spacing between actin and myosin varies at different sarcomere lengths (18). At rest length (ca. 2.70 μm) in rabbit psoas muscle, the surface-to-surface spacing between actin and myosin is greater than the largest lengths attributed to the S-1 moieties of myosin (16, 23, 25).

H. E. Huxley postulated that the subfragment-2 (S-2) moieties of myosin might function as hinges between the light meromyosin (LMM) backbones and the S-1 moieties of myosin. Therefore the movements of S-2 moieties away from the long axis of the myosin backbones would permit the attachment of the S-1 moieties at the same orienta-

tion to actin over a considerable range of filament spacings (17).

Huxley's suggestion that the S-2 moieties of myosin might angle away from the myosin long axis during the transition from relaxed to contracted or rigor state demands that the intrinsic birefringence of the myosin aggregates decrease (Fig. 1). If the S-2 moieties are capable of swinging out from the myosin long axis, then the amount of myosin oriented parallel to the long axis (slow crystalline axis) would decrease, resulting in a decrease in the intrinsic birefringence.

Conversely, the intrinsic birefringence would increase in the transition from rigor or contracted state to the relaxed state as the S-2 moieties of myosin returned to positions more parallel to the long axis of the myosin aggregates (Fig. 1). Therefore, definite structural changes would occur within the myosin aggregate during the rigor to relax transition. Recently, it has been demonstrated, to a first approximation, that the rigor to relax transition would involve an increase of intrinsic birefringence of ca. 4.0% or less if the S-2 moieties function as hinges (37).

Linear birefringence measurements have been successfully applied to the study of intact muscle. Vertebrate striated muscle has been characterized as containing highly birefringent anisotropic (A) bands and only weakly birefringent isotropic (I) bands (28). Huxley and Hanson (19) demonstrated that myosin was the birefringent protein of the A band, while Colby (8) quantified the variations of intrinsic birefringence along single myofibrils immersed in *o*-toluidine. Colby showed that the intrinsic birefringence in the region of actin and myosin overlap was much less than that of thin filaments alone. This result demonstrated that interactions between thick and thin filaments involved some loss of intrinsic birefringence.

Measurements of birefringence have also been used in studying the dynamics of muscle contraction (see reference 14 for review). Biphasic decreases in birefringence were measured classically during isometric contractions (39, 5), but Eberstein and Rosenfalck (10) demonstrated that monophasic decreases occurred in the absence of mechanical and optical artifacts. Eberstein and Rosenfalck (10) measured a decrease (ca. 5.0%) in total birefringence that reached a minimum before the tension reached a maximum at a sarcomere length of ca. 2.50 μm (rest length in frog muscle). It was suggested that the measured decrease in birefringence during isometric contraction might be due either to an increase in the number of "cross-links" between contractile elements or to a displacement of water in the fibers (10).

Four types of linear birefringence are present in muscle fibers. Form birefringence results from the presence of asymmetric isotropic or anisotropic particles oriented in a preferred direction in a medium with a different refractive index, i.e., S-1 moieties of myosin and actin. Pure form birefringence can be completely abolished by allowing the muscle to imbibe a fluid with a refractive index matching that of the particles (4, 8). Intrinsic

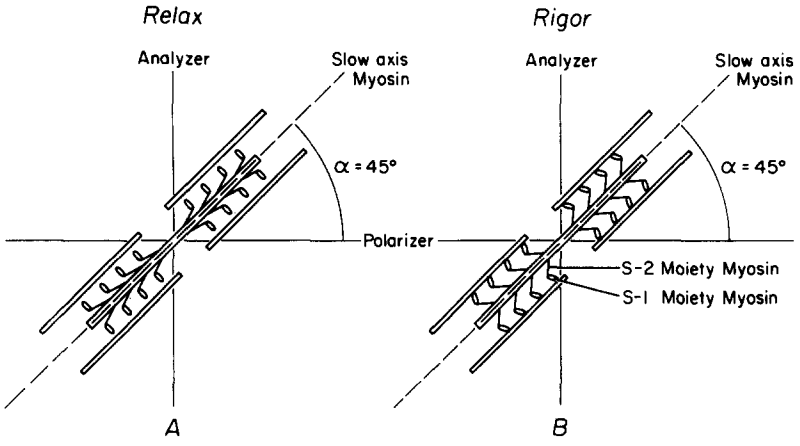

FIGURE 1 The structural changes of myosin after Huxley (17) during the rigor (B) to relax (A) transition. If the S-2 moiety of myosin functions as a hinge, then the positive intrinsic birefringence must increase during the transition. The slow axis of the myosin aggregate is parallel to the long axis and is shown here to be 45° to the transmission plane of the polarizer.

birefringence results from the asymmetrical arrangement of the polarizabilities of the chemical bonds, i.e., α-helical structure of LMM, tropomyosin, and S-2 moieties of myosin. This type of birefringence can not be altered by imbibition of a solution of matching refractive index. Strain birefringence results from strain due to the application of tension or compression. Strain birefringence may be due to either intrinsic or form birefringence depending on whether an amorphous medium or a partially organized asymmetric medium is strained. Edge birefringence occurs at the boundary between two materials with different refractive indexes. This type of birefringence can also be eliminated by immersion of the material in a medium of matching refractive index.

Useful information may be gained when the polarization properties of muscle are related to data derived from X-ray diffraction and electron microscopy (18, 24, 30–32). Polarized light techniques including linear birefringence, linear dichroism, difluorescence, and circular dichroism have the advantage that relatively small volumes may be measured during a short time interval. This property of polarized light techniques is particularly valuable in studying the dynamics of contraction within single muscle fibers, myofibrils, and nonmuscle motile systems.

It is the aim of this investigation to determine whether the changes in birefringence measured in the rigor to relax transition in rabbit psoas muscle fibers are compatible with the view that the S-2 moieties of myosin function as hinges between the S-1 moieties and LMM backbones of myosin. The present paper correlates the changes of birefringence with published information based on X-ray diffraction, electron microscopy, and other polarized light studies. The recent development of quantitative polarized light methods[1] (1, 2, 36, 38) and the ability to separate various polarization properties (36, 38) make it possible to quantify polarized light interactions in small volumes rapidly and reproducibly.

MATERIALS AND METHODS

Birefringence Measurements

The phase modulation microspectrophotometer (PM-MSP) measures various optical properties exhibited by complex anisotropic solids. The PM-MSP used here is an automatic photoelectric, null-seeking birefringence detection system. The original instrument described by Allen et al. (1) has been redesigned to facilitate spectral measurements of birefringence, linear dichroism and circular dichroism, optical rotatory disperson, and includes data reduction procedures for separating these polarization properties (36, 38).

The present investigation utilized the birefringence mode of the instrument and a Zeiss photomicroscope I equipped with selected strain-free polarization optics (Zeiss 16.0 ×, NA 0.32 objectives were used as objective and condenser) and conventional polarization accessories. A special substage has been constructed that accommodates the electro-optical light modulator (EOLM) which is a crystal of lithium niobate that modulates the phase of the light $\pm \lambda/20$. The polarizer is permanently mounted at the entrance to the substage with its plane of transmission (E vector) parallel to the vertical (North-South) axis.

The microscope is illuminated by a 150-W xenon arc source equipped with a Zeiss quartz monochromator (Carl Zeiss Corp., New York). It is also possible to use the phase randomized output of a 5-W argon ion or dye laser as a light source for applications requiring the ultimate in speed, sensitivity, or spectral purity.

Light passing through the portion of the muscle preparation where the measurements are made (ca. 10 sarcomeres) may be isolated by field aperture diaphragms (0.1–1.0 mm in diameter) and/or by apertures situated in a Zeiss photometer head sampling the image plane. Light passing through the sampling aperture falls on the photocathode of an end-window photomultiplier (EMI 9634 QB). A block diagram (Fig. 2) shows the relationships of the optical and electronic components of the system. The 3KC lock-in amplifier provides the signal for driving the EOLM, as well as detecting and demodulating the signal from the phototube amplifier. The AC signal from the photomultiplier is directed through a narrow band pass amplifier to the phase-sensitive detector which is sensitive only to the intensity fluctuations that coincide with the frequency and phase of the oscillator. The automatic compensator capabilities of the closed servo loop are utilized in the measurements of birefringence (1, 2). In addition, comparable measurements have been made with a new birefringence detection system that will be discussed elsewhere (see footnote one).

Data Acquisition and Calibration

In the birefringence mode the muscle preparations are introduced into the measuring beam (λ = 546 nm) whose diameter is limited to the diameter of the muscle fiber. The muscle is rotated at a constant speed of 1 rps on a centered stage while the signal from the lock-in amplifier in the servo loop is recorded (36, 38). In positions where zero signal is recorded, the crystalline axes of the positive

[1] A new birefringence detection system (Polar Eye: Custom Instrumentation, Ravena, New York) will be discussed elsewhere (Taylor, D. L., and R. Zeh).

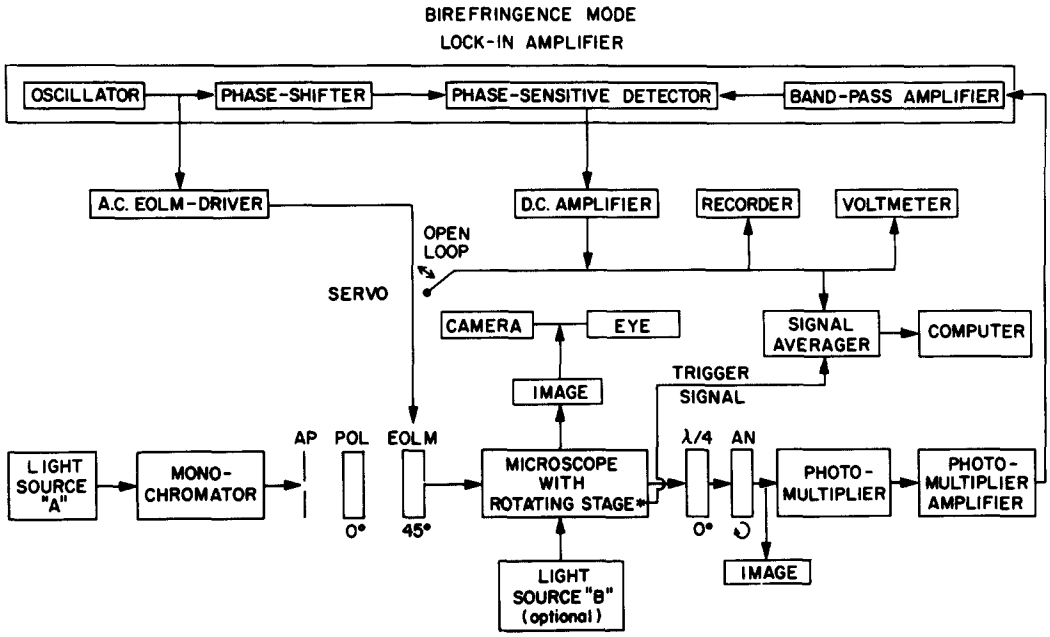

FIGURE 2 Diagram illustrating the optical and electronic components of the phase modulation microspectrophotometer.

birefringent muscle are parallel to the transmission axes of the analyzer and polarizer which were crossed. The orientation producing the maximum signal corresponds to that at which the crystalline axes are ±45° to the plane of the polarizer and parallel to the crystalline axes of the lithium niobate crystal (EOLM) (Fig. 3). Measurements are taken every 4° as the specimen is rotated on the stage, and there are four positions of extinction and maximum in a 360° rotation of the specimen. The signals are stored in a 100-point waveform eductor (Princeton Applied Research Corp., Princeton, N. J.) and plotted by means of an XY recorder or recorded on paper tape.

The quantity measured by the PM-MSP is the weighted mean phase retardation,

$$\Gamma = t\,(n_e - n_o) \qquad (1)$$

where t is the specimen thickness, n_e is the refractive index of the extraordinary ray, and n_o is he refractive index of the ordinary ray. The birefringence,

$$B = (n_e - n_o), \qquad (2)$$

was determined by dividing the phase retardation (Γ) by the thickness (t) of the specimen:

$$(n_e - n_o) = \frac{\Gamma}{t} \qquad (3)$$

It was assumed, in calculating the diameters, that the muscle fibers were cylindrical. In fact, most single fibers are slightly oval in cross section.

The calibration is performed in the absence of a specimen with an achromatic λ/4 plate inserted above the EOLM with its slow axis parallel to the plane of the polarizer. In this position the instrument reads zero phase retardation. When the analyzer is rotated clockwise and counterclockwise, the angular equivalents of positive and negative phase retardation are introduced as

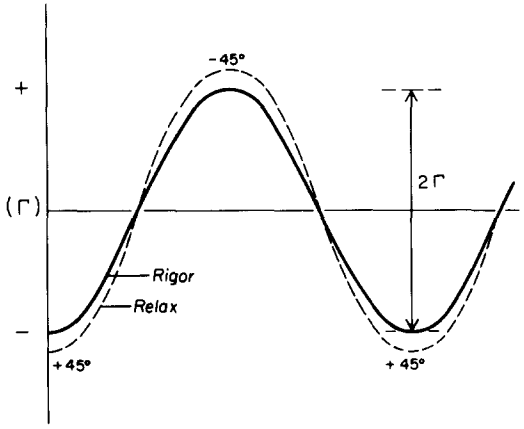

FIGURE 3 Sinusoidal variation in phase retardation (Γ) of rigor (——) and relaxed (----) single fibers during rotation on the microscope stage. The maximum phase retardation occurs when the crystalline axes of the fibers are 45° to the polarizer transmission plane. The increase in phase retardation (Γ) during the rigor to relax transition is symmetrical around zero.

in all applications of the classical de Senarmont compensator principle (4). The retardation in angstroms is equal to the number of degrees the de Sénarmont compensator is rotated multiplied by the wavelength of light in angstroms divided by 180°.

$$\Gamma = \frac{(\text{compensator rotation}) \times \lambda}{180^\circ} \quad (4)$$

The analyzer is set at the angle corresponding to a set of standard retardations, ie. 50, 100, 200, etc. The servo amplifier output is subsequently plotted for the standard phase retardation, and a standard curve is generated for comparison with the observed retardations of test specimens. The compensator is linear for one full wavelength.

Specimen Preparation

Bundles of rabbit psoas muscle were prepared with a rapid demembranating technique modified after Solaro et al. (34). Small strips of rabbit psoas muscle were prepared at different sarcomere lengths by stretching the resting muscle *in situ*. The psoas muscles were tied to wooden sticks and placed in the triton extraction solution for 6 h at 0°C. The triton extraction solution was subsequently replaced with a glycerol storage solution modified after Rome (30). The muscle was used anytime between 4 and 42 days after preparation. Single fibers were teased out of a bundle of muscle with fine watchmaker's forceps.

Several experiments were performed in order to measure the change in intrinsic birefringence in the transition from rigor to relaxed state. Single fibers were dissected out of a bundle and cut in half. One half of a single fiber was maintained in rigor solution while the other half was relaxed. The phase retardation of each half fiber was averaged as the fibers were scanned across their total lengths. The two matching fibers were then fixed for 2 h in 4% glutaraldehyde in rigor and relaxing solutions, respectively. After fixation the fibers were treated with increasing concentrations of dimethyl sulfoxide (DMSO) up to 100%. Subsequently, the solutions were replaced by 100% *o*-toluidine (n = 1.57), the refractive index which matched that of the muscle proteins (8). Then, the intrinsic birefringences were compared between rigor and relaxed fibers.

Solutions

The triton extraction solution consisted of 20 mM phosphate buffer, 80 mM KCl, 5.0 mM Ethyleneglycolbis[β-aminoethyl ether] N,N'-tetraacetic acid (EGTA), 2.5 mM dithiothreitol, and 1.0% Triton X-100, pH 7.0. The glycerol storage solution contained 20.0 mM phosphate buffer, 80 mM KCl, 5.0 mM EGTA, 2.5 mM dithiothreitol, and 50% glycerol, pH 7.0.

Rigor was maintained in a solution modified after Rome (32) (5.0 mM (PIPES) buffer, pH 7.0, 5.0 mM EGTA, 6.0 mM $MgCl_2$, and 98.0 mM KCl). The muscle fibers relaxed without shortening in 5.0 mM PIPES buffer, pH 7.0, 5.0 mM EGTA, 5.0 mM $MgCl_2$, 3.0 mM Na_2ATP, and 85 mM KCl. A pyrophosphate-relaxing solution was prepared by replacing the ATP in the standard relaxing solution with 3.0–5.0 mM pyrophosphate. The contraction solution consisted of the relaxation solution containing enough $CaCl_2$ to allow a total free calcium ion concentration of ca. 1.0×10^{-4} M.

The myosin was extracted from some of the muscle preparations by a procedure modified after Huxley and Hanson (19) (100 mM Pyrophosphate, 10 mM PIPES buffer, 1.0 mM $MgCl_2$, pH 7.0).

Experimental Procedure

The specimen chamber consisted of a pair of no. 0 cover slips held apart by an observation plate. The specimen chamber with the test solution was first rotated on the microscope stage to test for strain birefringence (<2 Å). The muscle fibers were tied at each end with fine strands of silk thread. One end was tied down, while the other end was attached to a lever that controlled the fiber length. Care was taken to orient the single fibers without applying a strain to the rigor muscle. The muscle fibers were rotated on a motor-driven stage while the sinusoidal fluctuation of phase retardation was recorded (Fig. 3). Less than a 2.0% increase or decrease in fiber diameter occurred during the experiments. After the phase retardation of rigor muscle fibers was measured, the perfusion chamber volume was rapidly exchanged with relaxation solution, and the measurements were repeated. The fiber positions, the sarcomere lengths, and the fiber diameters were monitored before and after relaxation by photographing the specimens. All experiments were discarded in which there occurred visible sarcomere disorganization, changes in sarcomere length of more than 2.0%, changes in fiber diameter of more than 2.0%, or fibers that failed to contract when placed in contraction solution (relaxation solution with the addition of calcium to a final free calcium concentration $> 1.0 \times 10^{-6}$ M) at the end of the experiment. The studies were performed at room temperature (21–24°C).

Calculation of Birefringence

Wiener's equation (41) predicts the dependence of form birefringence on the refractive index of the medium (n_m), a single refractive index for the component rods (n_p), and the volume fraction of the rods (ϕ_p) and medium (ϕ_m). Birefringence is determined by the difference between the refractive indices of the extraordinary and ordinary rays. However, the Wiener formulation is given as the difference of the squares of the refractive indices:

$$n_e^2 - n_o^2 = \frac{\phi_p \phi_m (n_p^2 - n_m^2)^2}{(1 + \phi_p) n_m^2 + \phi_m n_p^2} \quad (5)$$

The Wiener formula can be used to a first approximation as:

$$(n_e - n_o) = \frac{\emptyset_p \emptyset_m (n_p^2 - n_m^2)^2}{(n_e + n_o)[(1 + \emptyset_p) n_m^2 + \emptyset_m n_p^2]} \quad (6)$$

$n_e + n_o$ can be substituted by:

$$(n_e + n_o) = 2(\emptyset_p n_p + \emptyset_m n_m). \quad (7)$$

Therefore, the Wiener equation assumes the form:

$$(n_e - n_o) = \frac{\emptyset_p \emptyset_m (n_p^2 - n_m^2)^2}{2(\emptyset_p n_p + \emptyset_m n_m)[1 + \emptyset_p) n_m^2 + \emptyset_m n_p^2]} \quad (8)$$

The volume fraction of filaments in vertebrate striated muscle has been determined in various ways (7). Recently, Sato et al. (33) have determined the volume fraction of filaments by measuring the cross-sectional dimensions observed in electron micrographs. The volume fraction of filaments was determined to fall within a range between 0.041 and 0.086. A value of 0.064 was found as the "best fit" curve (33). The refractive index of the filaments has been determined classically to be equal to 1.57 (8, 28), while a refractive index of 1.33 has been used for the medium.

The Wiener equation only describes the form birefringence, and the intrinsic birefringence is determined by having the specimens imbibe a medium of matching refractive index (3, 8, 28, 33). The ratio of form to intrinsic birefringence has been reported over a range from 1.5:1 to 2:1 (12, 28).

Preparation of Synthetic Myosin Filaments

Myosin was extracted from rabbit psoas muscle according to the procedure described by Kielly and Harrington (21). The purified myosin was dissolved in 0.5 M KCl, 10.0 mM imidazole buffer, pH 7.0, and diluted to a final concentration of 3.7 mg/ml. Then myosin filaments were formed by rapid dilution according to a procedure modified after Kaminer and Bell (20). The filaments formed on dilution to 0.1 M KCl with 10.0 mM imidazole buffer, pH 7.0. The protein concentration was subsequently diluted to 0.19 mg/ml. 2 ml aliquots of the filament suspensions were dialyzed against rigor and relaxing solutions for 3 h. The rigor solution contained 0.1 M KCl, 1.0 mM EGTA, 2.0 mM $MgCl_2$ and 10.0 mM imidazole, pH 7.0. The relaxing solution contained 2.0 mM ATP in addition to the rigor solution, pH 7.0.

Negative Staining

A drop of each sample was applied to a Formvar carbon-coated grid and treated according to the technique described by Moore et al. (26).

Electron Microscopy

A Philips EM 301 was used with an acceleration voltage of 80 kV, a 300 μm condenser aperture, and a 50 μm objective aperture.

RESULTS

Birefringence of Muscle Fibers and Myofibrils in Rigor

The average total birefringence of 27 single fibers at a sarcomere length of 2.70 μm was $(1.46 \pm 0.08) \times 10^{-3}$, assuming that the thickness was equal to the fiber diameter. The total birefringence of rigor muscle fibers was dependent on sarcomere length and ranged from $(1.46 \pm 0.08) \times 10^{-3}$ to $(1.60 \pm 0.04) \times 10^{-3}$ at sarcomere lengths from 2.70 μm to 3.40 μm (ca. 10.0% increase). The total birefringence decreased to $(4.0 \pm 0.5) \times 10^{-4}$ after the myosin was extracted (ca. 10% nonmyosin protein is also extracted with the pyrophosphate myosin extraction procedure [19]).

Increase in Birefringence During the Transition from Rigor to Relaxed State

An increase in birefringence was measured dependent on sarcomere length when 55 single fibers were relaxed from the rigor state with Mg-ATP. The total birefringence at rest length (ca. 2.70 μm) was $(1.67 \pm 0.05) \times 10^{-3}$, or ca. 14.0% greater than that of rigor fibers. The increase in total birefringence during Mg-ATP relaxation was smaller at longer sarcomere lengths where there was a decrease in actin and myosin overlap as well as a decrease in lattice spacing (Fig. 4). No change in birefringence wes detected upon the addition of the Mg-ATP-relaxing solution after the myosin was extracted.

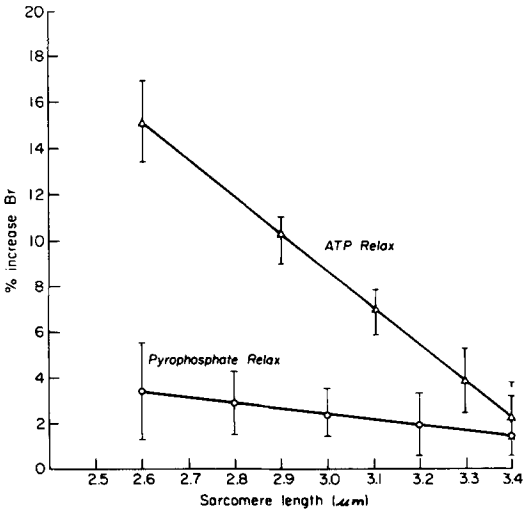

FIGURE 4 Percent increase in birefringence during the rigor to ATP relax (Δ——Δ) and pyrophosphate relax (O—O) at various sarcomere lengths.

Increase in Birefringence During the Transition from Rigor to Pyrophosphate-Relaxed State

Pyrophosphate relaxation produced a smaller increase in retardation compared to Mg-ATP (Fig. 4). At rest length, pyrophosphate relaxation increased the total birefringence by ca. 3.0%, and no further increase in birefringence was observed by increasing the magnesium and pyrophosphate concentrations to 10.0 mM.

Stepwise Increase in Birefringence During the Transition from Rigor to Pyrophosphate-Relaxed to ATP-Relaxed States

Muscle fibers relaxed for less than 5 min in pyrophosphate increased in birefringence after the addition of the Mg-ATP-relaxing solution (Fig. 5). There was a greater increase in birefringence in rest-length fibers than in fibers with longer sarcomere lengths (Fig. 5 *A* and *B*).

Changes in Birefringence by Varying the Lattice Spacing

The lattice spacings of single relaxed fibers (actin to myosin interfilament distances) were changed by varying the pH and ionic strength of the bathing media in order to determine the effect of varying the lattice spacing on the total change in birefringence (30, 31). Rome (31) demonstrated that there was an increase in the actin-to-myosin lattice spacing when the pH of the media was increased from pH 6.3 to pH 7.0. In the present case, the increase in lattice spacing caused a 2.0% increase in the diameter of the fibers. Wiener's equation predicts a ca. 4.0% decrease in form birefringence, while the measured decrease in birefringence was 5.0%.

Relaxed muscle fibers contracted when the pH of the relax solutions was changed from pH 7.0 to pH 7.7. Waves of contractions passed up and down the attached fibers.

Rome also demonstrated that the actin-to-myosin lattice spacing decreased as the ionic strength increased or when muscle fibers with sarcomere lengths greater than 2.70 μm were relaxed (31). The muscle fiber diameters decreased by 2.0% at a sarcomere length of 2.90 μm when the ionic strength was increased from 0.04 to 0.14 or when the fibers were relaxed with Mg-ATP. Perturbing the relaxed fibers by increasing the ionic strength of the bathing medium caused an increase in birefringence close to that predicted by changes in form birefringence (Table I). Conversely, there was almost a twofold increase in birefringence during the rigor to relax transition as compared to the experiments in which the ionic strength of the bathing medium was increased

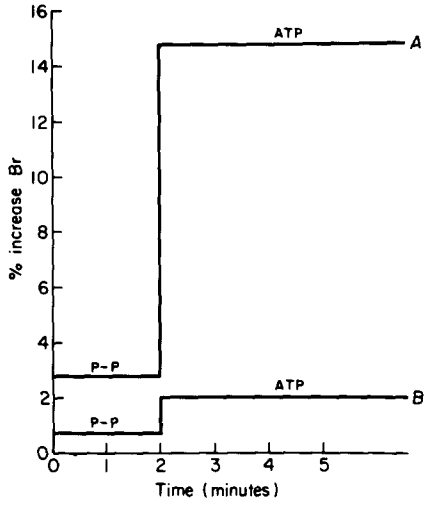

FIGURE 5 Percent increase in birefringence during the rigor to pyrophosphate relax (P-P) and subsequent ATP relax (ATP). Fibers at rest length (2.70 μm) (A) and (3.4 μm) (B).

TABLE I

Effect of Lattice Spacing Changes and Mg-ATP Relaxation on the Birefringence of Muscle Fibers. Sarcomere length 2.9 μm, pH 7.0

Treatment	Change in fiber diameter	Change in birefringence	Change in form birefringence predicted from Wiener's equation
	%	%	%
Increase of ionic strength from 0.04 to 0.14*	−2.0	+3.2 ± 0.5	+4.0
Rigor to relax (Mg-ATP)	−2.0	+9.0 ± 0.8	+4.0

* Muscle fibers were initially relaxed and then the ionic strength of the relaxing solutions was varied from 0.04 to 0.14.

(Table I). A comparison of the changes in birefringence during these separate experimental treatments demonstrates that the changes in lattice spacings alone do not account for the total changes in birefringence during relaxation (Table I).

Increase in Intrinsic Birefringence in the Transition from the Rigor to Relaxed State

The intrinsic birefringence of relaxed muscle fibers was compared to that of muscles in rigor. The phase retardations of rigor and relaxed fibers were compared before and after imbibition of a medium of matching refractive index. Initially, bisected muscle fibers at a sarcomere length of 2.9 μm possessed the same average phase retardation. Following relaxation, the phase retardation and birefringence increased by 9.0%. Fixation of both the rigor and relaxed muscle fibers caused approximately the same percent decrease in total phase retardation. During relaxation, the intrinsic birefringence increased by 4.8%, while the form birefringence increased by 4.2% (Table II).

Comparison of Measured Birefringence and Calculated Birefringence in Muscle Fibers

The calculated form birefringence varies according to the $\emptyset_p$ and n_p used in the equation. Classically, the $\emptyset_p$ has been measured around 0.1 while the n_p has been measured as ca. 1.57 (28). Therefore, Wiener's equation predicted a much larger birefringence than that measured (Table III). The birefringence of single muscle fibers has been measured over a range from 1.70×10^{-3} (6)

TABLE II

Changes of Intrinsic and Form Birefringence in the Rigor to Relax Transition

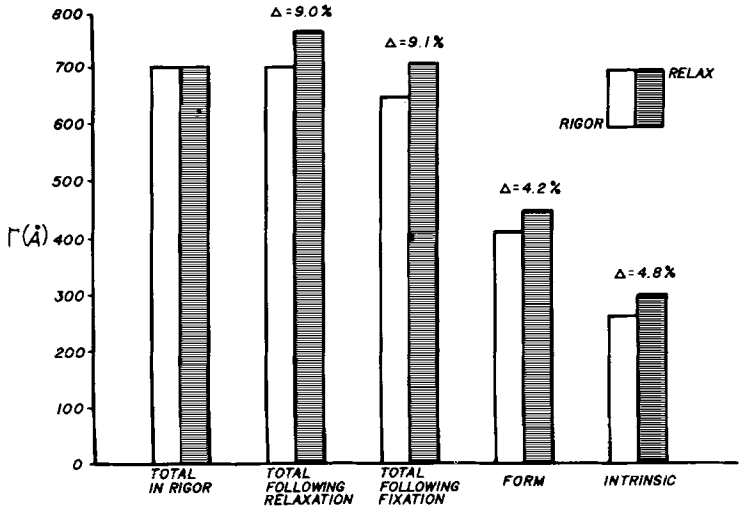

TABLE III

Birefringence of Single Muscle Fibers Calculated Using the Wiener's Equation

Form birefringence $\times (10^{-3})$ based on Wiener's Equation	$\emptyset_p$	n_p	Total Birefringence* $\times (10^{-3})$
5.40	0.15	1.57	8.10
3.81	0.10	1.57	5.72
2.74‡	0.07	1.57	4.11
1.91‡	0.07	1.53	2.87
1.68§	0.06	1.53	2.52

*The total birefringence is calculated by adding a component of intrinsic birefringence equal to one half the form birefringence (ratio of form to intrinsic birefringence is 2:1).
‡ The $\emptyset_p$ ("best fit") determined by Sato et al. (33).
§ The smallest probable $\emptyset_p$ (33).

to 2.30×10^{-3} (11), while the present experiments indicated that triton-extracted fibers had a total birefringence of $(1.67 \pm 0.05) \times 10^{-3}$. The triton extraction procedure might account for the differences observed in the present experiments.

Conversely, Sato et al. (33) have demonstrated recently that the $\emptyset_p$ is less than 0.1, and their best fit Wiener curves indicate that the n_p should be slightly less than 1.57. They have suggested that a gradual imbibition procedure could eliminate irreversible damage to proteins. Table III presents the form birefringence calculated by Wiener's equation for a series of possible $\emptyset_p$ and n_p values. The last column in Table III lists the total birefringence after correction for intrinsic birefringence if one assumes a ratio of form birefringence to intrinsic birefringence of 2:1 (7). The smallest possible total birefringence determined is ca. 33.0% greater than that measured for rest length relaxed fibers in the present study and is only ca. 0.08% greater than the birefringence measured by Fischer (11).

Structure of "Rigor" and "Relaxed" Synthetic Myosin Filaments

Significant differences were observed between synthetic myosin filaments dialyzed against rigor and relaxing solutions. 93% of the 483 relaxed filaments observed in seven different grid preparations were spindle shaped with no well defined bare central zone. The filaments had a mean length of 1.03 μm with a SD of 0.08 μm (Fig. 6). In contrast, 78% of the 626 rigor filaments observed in 10 different grid preparations had gross irregular projections at both ends with distinct bare

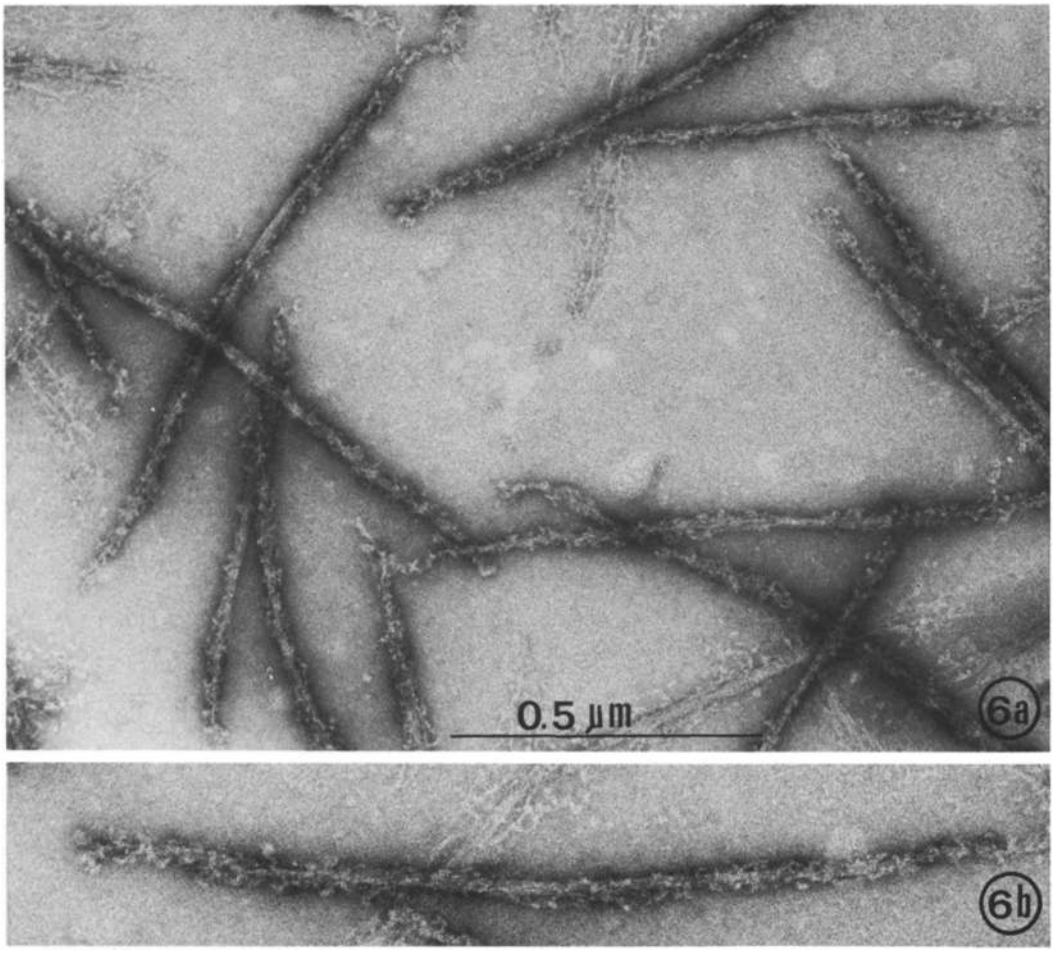

FIGURE 6 (*a*) Spindle-shaped myosin aggregates with no bare central zones were found predominantly in relaxing solution. × 34,000. (*b*) Higher magnification of a single relaxed filament. × 58,000.

central zones. The rigor filaments were of the same size as the relaxed filaments with a mean length of 1.04 μm and a SD of 0.10 μm (Fig. 7). These observations are almost identical to those made by Kaminer and Bell (20) who compared filaments formed on dilution to various ionic strengths and pH's.

DISCUSSION

Evidence that the Change in the Null Point of the PM-MSP in the Transition from Rigor to Relaxed State is a Measure of the Change in Birefringence

Changes in the light intensity passing crossed polars during the transition from the rigor to the relaxed state may arise from a change: (*a*) in the path length due to changes in muscle orientation and/or diameter, (*b*) in diffraction properties (10), (*c*) in depolarization scattering (10), (*d*) in absorption, (*e*) in the strain birefringence (stretch or compression), or (*f*) in form birefringence and/or intrinsic birefringence.

The gross orientation of the muscle preparations was controlled by rotation of the muscle during the course of the experiments. Any slight lateral reorientation of the muscle fiber during the addition of test solutions caused only a small phase shift in the signal (Fig. 3). Furthermore, the area of the muscle measured was photographed before and after each experiment. Fibers which became disorganized or whose sarcomere length changed by more than 2.0% were discarded. Changes in the

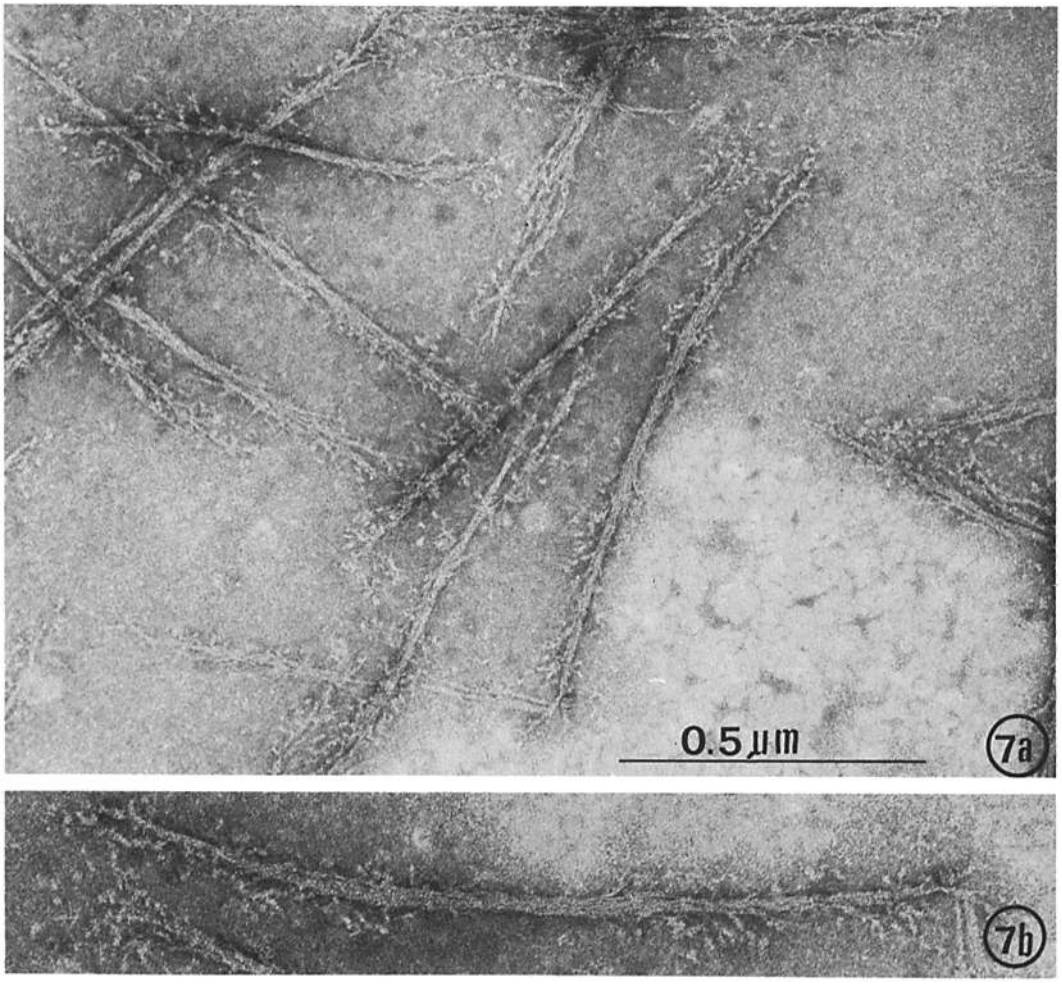

FIGURE 7 (*a*) Myosin aggregates with gross irregular projections at either end and clearly defined bare central zones were found predominantly in rigor solutions. × 34,000. (*b*) Higher magnification of a single rigor filament. × 58,000.

light intensity of unpolarized light in the rigor to relax transition were less than 0.5% and were independent of specimen orientation. Therefore, diffraction and absorption changes were not large in the present measurements. Changes in light intensity due to depolarization light scattering would disappear after immersion in a medium of matching refractive index. In addition, these effects would not show four angles of extinction and maximum in a 360° rotation as observed. Strain birefringence was avoided by the careful attachment of single fibers in the experimental chamber. Furthermore, the PM-MSP was designed to minimize the effects of light scattering, absorption, fluctuations in source intensity, and stray light. The fluctuation of the light intensity due to the addition and subtraction of ca. $\lambda/20$ to the specimen is recorded as the voltage required to drive a linear compensator to null in a servo loop (1). The PM-MSP in the birefringence mode responds to compensatable ellipticity introduced by the specimen. The muscle preparations showed four positions of extinction and maximum intensity during a 360° rotation which is characteristic of birefringent specimens (Fig. 3 depicts 180° rotation of the specimen). It is concluded that the changes in light intensity detected by the PM-MSP in these experiments are related primarily to changes in birefringence.

Molecular Basis of the Variation of Muscle Fiber Birefringence

The total birefringence of muscle fibers depends on a combination of form and intrinsic birefringence components. The form birefringence depends on the lattice spacing (volume fraction of filaments) and the organization of the filaments within the muscle fiber. The form birefringence of muscle fibers should vary in a competing fashion at increasing sarcomere lengths. The number of overlapped actin and myosin filaments per unit length will decrease as actin filaments are withdrawn from the A band. A decrease in the number of filaments would tend to diminish the total form birefringence. On the other hand, the lattice spacing of the filaments decreases at longer sarcomere lengths to maintain the constant volume characteristic of vertebrate striated muscle. Therefore, the form birefringence would increase depending on the increased volume fraction of filaments. In addition, other structures within the muscle fibers, i.e., S-1 moieties of myosin, that might change orientation could alter the form birefringence.

The intrinsic birefringence of muscle is due primarily to the myosin filaments (LMM and S-2 moieties) and secondarily to tropomyosin. The intrinsic birefringence could vary in muscle fibers if portions of the intrinsically birefringent contractile proteins changed conformation or orientation. For example, tropomyosin is believed to change position within the actin helix by slight "rolling" movements (35). These movements should not affect the intrinsic birefringence greatly, while large variations in the whole actin backbone as suggested by Oosawa (29) could alter the orientation of tropomyosin. However, X-ray diffraction measurements indicate that actin is a rather invariant structure (17).

If the S-2 moieties of myosin function as hinges in spanning the interfilament space between myosin and actin, then the intrinsic birefringence of the myosin aggregates in rigor would be maximal at longer sarcomere lengths where the interfilament distance decreases (S-2 moieties parallel to LMM backbones, Fig. 1) and minimal at shorter sarcomere lengths where the interfilament distance is largest (S-2 moieties angled away from the LMM backbones, Fig. 1).

It has been shown (37) that the total birefringence increases less with increasing sarcomere lengths in relaxed muscle fibers than in rigor fibers (11). Since Colby (8) found a decrease in intrinsic birefringence in the region of actin and myosin overlap in myofibrils in rigor, it is reasonable to suggest that the angular movements of the S-2 moieties of myosin are involved.

The increase in birefringence in the rigor to relax transition is compatible with the view that the S-2 moieties of myosin function as hinges (17). The dependence of sarcomere length on the amplitude of the increase of total birefringence in the rigor to relax transition could be explained equally well by one or a combination of two possibilities. First, the amount of actin and myosin overlap could control the number of crossbridges initially angled away from the long axis of the myosin aggregates. A decrease in the actin and myosin overlap would decrease the number of crossbridges initially angled in rigor. Therefore, the relaxation at longer sarcomere lengths would affect a smaller percentage of the total crossbridges. This possibility requires that the actin overlap control the movements of myosin directly. Secondly, at increasing sarcomere lengths the angular movement of S-2 moieties would decrease since the lattice spacing decreases. As the lattice spacing decreases, the S-2 moieties would not have to move out as far to

reach actin, and the change of angle in the transition from rigor to relaxed state would be smaller at longer sarcomere lengths. This latter possibility does not require actin to affect the movements of myosin directly.

The pyrophosphate relaxation experiments indicate that the dissociation of the actin and myosin alone does not cause a large increase in the birefringence of the muscle fibers (Fig. 4). The small increase in measured birefringence could be explained by the minimal movement of S-2 moieties induced by pyrophosphate relaxation. This interpretation is consistent with the results obtained by White (40) who characterized the pyrophosphate relaxation as a reduction in tension without a decrease in stiffness in comparison to rigor. It was suggested that the crossbridges remain in close proximity but not attached to the actin filaments. Furthermore, Lymn and Huxley (24) showed by X-ray diffraction that pyrophosphate did not cause a complete loss of the rigor crossbridge pattern. This indicates that the S-1 moieties and actin are in a continued close proximity. The stepwise increase of birefringence from rigor to pyrophosphate relaxation to ATP relaxation (Fig. 5) is consistent with the view that the S-2 moieties return to the resting position after myosin binds Mg-ATP (17, 18).

Rome (31, 32) demonstrated that the actin to myosin lattice spacing decreased as the ionic strength increased or when glycerinated muscle fibers at sarcomere lengths greater than 2.70 μm were relaxed (32). It has been shown (Table I) that muscle fibers (2.90 μm sarcomere length) decreased in diameter by 2.0% when the ionic strength of the relaxing solution was increased from 0.04 to 0.14 or when fibers in rigor were relaxed with Mg-ATP. Perturbing the relaxed fibers by increasing the ionic strength of the bathing medium caused an increase in birefringence close to that predicted by the changes in form birefringence. However, the rigor to relax transition, which involved the same slight change in fiber diameter, exhibited almost twice the increase in total birefringence as compared to the ionic strength control (Table I). Therefore, changes in the lattice spacing alone could not account for the total increase in birefringence during relaxation.

It is interesting that increasing the pH of relaxed fibers from pH 7.0 to pH 7.7 caused wavelike contractions in the absence of calcium. This increase in pH would increase the interfilament spacing which should tend to decrease the chance for myosin-actin interactions. However, Kaminer and Bell (20) demonstrated that synthetic myosin aggregates have drastically different structures depending on the pH and/or ionic strength of the medium. In the presence of 0.1 M KCl the filaments were spindle shaped at a pH of 7.0, but they exhibited gross irregular projections at pH 8.0. If the gross irregular projections observed on the myosin aggregates are the S-2 moieties of myosin, then the increase of pH in the intact, relaxed fibers could cause the outward movement of the crossbridges. This process could allow the interaction between myosin and actin. Transient interactions could occur since the fibers were bathed in an ATP-containing relaxing solution.

Changes in Intrinsic Birefringence

The increase in birefringence upon relaxation with Mg-ATP involves an increase in intrinsic birefringence as well as form birefringence. Since the S-2 moieties are rods containing ca. 90.0% α-helices (22) they are birefringent, while the S-1 moieties are practically optically isotropic. A complete investigation relating the changes of the intrinsic birefringence to sarcomere length has not been completed, but initial measurements indicate that ca. half the total increase in birefringence during relaxation is due to intrinsic birefringence. A new method of imbibition (33) is currently being used to optimize the physical stability of the specimens.

Recently, the changes in intrinsic birefringence have been calculated in the rigor to relax transition, assuming a hinge function of the S-2 moieties (37). At rest length, the maximum predicted increase of intrinsic birefringence is ca. 4.0%. Since the intrinsic birefringence accounts for approximately half the increase in total birefringence during the rigor to relaxation transition, then the measured changes in birefringence fit reasonably with the predicted value (Fig. 8). However, the measured changes in birefringence are slightly greater than the maximum predicted value (37). It is possible that other structural changes such as the "rolling"movements of tropomyosin (17, 35) as well as conformational changes within the myosin backbone (13) affect the changes in intrinsic birefringence. These latter possibilities are being investigated.

Can Birefringence Measurements Determine Contractile State?

A comparison of the sign and amplitude of the changes in birefringence in muscle fibers during contraction and relaxation indicates that the position of the total crossbridges can be monitored. Eberstein and Rosenfalck (10) measured a ca. 5.0% decrease in total birefringence in isometrically contracting frog muscle fibers at rest length (ca 2.5 μm). The percent decrease in retardation decreased at longer sarcomere lengths, but slight decreases in retardation were still recorded at nonoverlap sarcomere lengths. If it is assumed that the frog muscle and rabbit muscle experiments can be compared, then the differences in the amplitudes of birefringence changes for contraction and relaxation are important. However, it must be pointed out that Eberstein and Rosenfalck (10) used freshly isolated single frog muscles and that the present investigation utilized triton-extracted, glycerinated rabbit psoas muscle. The difference between a ca. 5.0% decrease in total birefringence preceding isometric contraction (10) and a ca. 15.0% (half of it being intrinsic birefringence) increase in total birefringence in the rigor to relaxation transition at rest length could be explained by the fact that a maximum number of crossbridges are angled in rigor and that relaxation of glycerinated rabbit muscle gives a more complete detachment of the crossbridges than is observed in living muscle. In addition, the slight decreases in the diameters of glycerinated muscle fibers during relaxation probably account for part of the observed increase in the form birefringence.

Eberstein and Rosenfalck (10) measured a small decrease in birefringence even at nonoverlap sarcomere lengths, which suggests that a small number of crossbridges are activated in the absence of actin. However, the difficulty in assuring complete nonoverlap in whole muscle fibers makes this interpretation incomplete at this time.

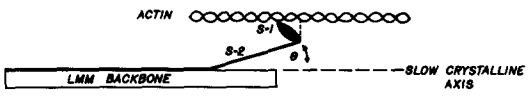

FIGURE 8 Model of the interaction between a single myosin molecule (part of a myosin aggregate) and an actin filament, assuming a hinge function of the S-2 moiety. The slow crystalline axis of the myosin aggregate is labeled. The angle θ depends on the interfilament spacing and the chemical state of the muscle (37).

The sign and amplitude of birefringence measurements can be used to identify the contractile state of muscles. Isometric contraction is preceded by a decrease in total birefringence, while relaxation from the rigor state causes an increase in total birefringence. Furthermore, the amplitude of the birefringence is dependent on the sarcomere length.

Structure of Synthetic Myosin Filaments

H. E. Huxley described the structure of synthetic myosin filaments as either spindle shaped or "spread" (gross irregular projections at either end). However, no apparent difference was noted in negatively stained preparations after the addition of low concentrations of ATP (16). Subsequently, Kaminer and Bell characterized synthetic myosin aggregates formed by varying the ionic strength and pH of the myosin solutions during filament formation (20). Filaments formed at an ionic strength of 0.1 M KCl had different structures depending on the pH. At pH 8.0, the filaments had gross irregular projections at both ends and a bare central zone. In contrast, at pH 7.5 the filaments had less prominent projections at the ends, and at pH 6.5 the filaments were spindle shaped and lacked well defined central zones. The filaments had a mean length of ca. 1.0 μm in 0.1 M KCl at pH 7.0.

The present experiments demonstrate that two distinct types of filaments can be formed at a constant pH and ionic strength by inducing either rigor or relaxation chemical conditions. The spindle-shaped filaments are observed at a higher frequency under relaxing conditions, while the spread-shaped (gross irregular projections) filaments are observed more readily under rigor conditions. However, both types of filaments were observed under the same conditions. The irregular projections observed in filaments treated with the rigor solution, and infrequently with relaxing solution, could be the S-2 moieties of myosin which could move to positions parallel to the long axis of the filaments during "relaxation." Under the latter conditions, spindle-shaped filaments would be observed more readily. The identification of the projections as the flexible "linkage" between the S-1 moieties and LMM of myosin requires further investigation. Synthetic and natural thick filaments under different conditions are being characterized presently by several physical properties. It

is interesting that both spindle- and spread-shaped myosin filaments are also observed in negatively stained preparations of amoeba cytoplasm (26).[2] The physiological implications are being investigated.

The complementary birefringence data from isometrically contracting (10) and relaxed single muscle fibers, as well as the structure of relaxed and rigor synthetic filaments, are consistent with the hypothesis that the S-2 moieties of myosin function as hinges to permit the attachment of S-1 moieties to actin.

Further studies will include rapid measurements of various polarization properties in isometrically contracting muscle fibers and the measurement of specific changes occurring within individual I bands and A bands. Emphasis will center on measuring the structural changes of specifically labeled components within different muscle types, isolated proteins, and nonmuscle motile systems.

I would like to thank R. D. Allen, R. E. Stephens, R. Lucas, S. Inoué, F. Walz, E. Salmon, J. Fuseler, A. F. Huxley, and D. Branton for helpful discussions. I am also indebted to R. Zeh, R. Speck, R. Loos, S. A. Hammond, and M. Adamian for valuable technical assistance. Dr. H. Sato et al. kindly placed unpublished data at my disposal (33).

This work was supported by research grants AM 18111 from the National Institute of Arthritis, Metabolism, and Digestive Diseases to D. L. Taylor, and GM 18854 from the National Institute of General Medical Science to R. D. Allen. These studies were initiated at the State University of New York at Albany, were extended while D. L. Taylor was a research associate at the Woods Hole Marine Biological Laboratory, and were completed at the Biological Laboratories, Harvard University.

Received for publication 30 June 1975, and in revised form 6 October 1975.

REFERENCES

1. ALLEN, R. D., J. W. BRAULT, and R. D. MOORE. 1963. A new method of polarization microscopic analysis. I. Scanning with a birefringence detecting system. *J. Cell Biol.* **18**:223–235.
2. ALLEN, R. D., J. W. BRAULT, and R. ZEH. 1966. Image contrast and phase modulation light methods in polarization and interference microscopy. *In* Advances in Optical and Electron Microscopy Vol. I. R. Barer and V. E. Cosslett, editors. Academic Press, Inc., New York. 77–114.
3. AMBRONN, H., and A. FREY. 1926. Das Polarisationsmikroskop. Akademische Verlagsgesellschaft mbH. Frankfurt.
4. BENNETT, H. S. 1950. Methods applicable to the study of both fresh and fixed materials. *In* McClungs Handbook of Microscopical Technique. R. McClung Jones, editor. Hoeber, Medical Division of Harper and Row, Publishers, New York. 591–677.
5. BOZLER, E., and C. L. COTTRELL. 1937. The birefringence of muscle and its variation during contraction. *J. Cell Comp. Physiol.* **10**:165–182.
6. BUCHTHAL, F., G. G. KNAPPEIS, and T. SJOSTRAND. 1939. *Skand. Arch. Physiol.* **82**:225–241.
7. CASSIM, J. Y., P. S. TOBIAS, and E. W. TAYLOR. 1968. Birefringence of muscle proteins and the problems of structural birefringence. *Biochim. Biophys. Acta.* **168**:463–471.
8. COLBY, R. H. 1971. Intrinsic birefringence of glycerinated myofibrils. *J. Cell Biol.* **51**:763–771.
9. DOSREMEDIOS, C. G., R. G. C. MILLIKAN, and M. F. MORALES. 1972. Polarization of tryptophan fluorescence from single striated muscle fibers. *J. Gen. Physiol.* **59**:103–120.
10. EBERSTEIN, A., and A. ROSENFALCK. 1963. Birefringence of isolated muscle fibers in twitch and tetanus. *Acta Physiol. Scand.* **57**:144–166.
11. FISCHER, E. 1944. The birefringence of striated and smooth mammalian muscles. *J. Cell Comp. Physiol.* **23**:113–130.
12. FISCHER, E. 1947. Birefringence and ultrastructure of muscle. *Ann. N. Y. Acad. Sci.* **47**:783–795.
13. HASELGROVE, J. C. 1975. X-ray evidence for conformational changes in the myosin filaments of vertebrate striated muscle. *J. Mol. Biol.* **92**:113–125.
14. HUXLEY, A. F. 1957. Muscle structure and theories of contraction. Progress in Biophysics and Biophysical Chemistry. Pergamon Press, Inc. Elmsford, N.Y. 255–318.
15. HUXLEY, A. F., and R. M. SIMMONS. 1971. Proposed mechanism of force generation in striated muscle. *Nature (Lond.)* **233**:533–538.
16. HUXLEY, H. E. 1963. Electron microscopic studies on the structure of natural and synthetic protein filaments from striated muscle. *J. Mol. Biol.* **7**:281–208.
17. HUXLEY, H. E. 1969. The mechanism of muscle contraction. *Science (Wash. D. C.).* **164**:1356–1366.
18. HUXLEY, H. E., and W. BROWN. 1967. The low-angle x-ray diagram of vertebrate striated muscle and its behavior during contraction and rigor. *J. Mol. Biol.* **30**:383–434.
19. HUXLEY, H. E., and J. HANSON. 1957. Quantitative studies on the structure of cross-striated myofibrils. I. Investigations by interference microscopy. *Biochim. Biophys. Acta.* **23**:229–249.
20. KAMINER, B., and A. L. BELL. 1966. Myosin filamentogenesis: effects of pH and ionic concentrations. *J. Mol. Biol.* **20**:391–401.

[2] Taylor, D. L. 1975. Unpublished results.

21. KIELLY, W. W., and W. F. HARRINGTON. 1960. A model for the myosin molecule. *Biochim. Biophys. Acta.* **41**:401–421.
22. LOWEY, S., L. GOLDSTEIN, C. COHEN, and S. M. LUCK. 1967. Proteolytic degradation of myosin and the meromyosins by a water-insoluble polyanionic derivative of trypsin. *J. Mol. Biol.* **23**:287–295.
23. LOWEY, S., H. S. SLAYTER, A. G. WEEDS, and H. BAKER. 1969. Substructure of the myosin molecule. I. Subfragments of myosin by enzymatic degradation. *J. Mol. Biol.* **42**:1–29.
24. LYMN, R. W., and H. E. HUXLEY. 1972. X-ray diagrams from skeletal muscle in the presence of ATP analogs. *Cold Spring Harbor Symp. Quant. Biol.* **37**:449–453.
25. MENDELSON, R. A., M. F. MORALES, and J. BOTTS. 1973. Segmental flexibility of the S-1 moiety of myosin. *Biochemistry.* **12**:2250–2256.
26. MOORE, P. L., J. S. CONDEELIS, D. L. TAYLOR, and R. D. ALLEN. 1973. A method for the morphological identification of contractile filaments in single cells. *Exp. Cell Res.* **80**:493–495.
27. NIHEI, T., R. A. MENDELSON, and J. BOTTS. 1974. Use of fluorescence polarization to observe changes in attitude of S-1 moieties in muscle fibers. *Biophys. J.* **14**:236–242.
28. NOLL, D., and H. H. WEBER. 1934. Polarisationsoptik und molekularer Feinbau der Z-Abschnitte des Froschmuskels. *Pfluegers Archiv Gesamte Physiol. Menschen Tiere.* **235**:234–246.
29. OOSAWA, F. 1975. Abstract of the Second International Congress of Biorheology. 37.
30. ROME, E. 1967. Light and X-ray diffraction studies of the filament lattice of glycerol extracted rabbit psoas muscle. *J. Mol. Biol.* **27**:591–602.
31. ROME, E. 1968. X-ray diffraction studies of the filament lattice of striated muscle in various bathing media. *J. Mol. Biol.* **37**:331–344.
32. ROME, E. 1972. Relaxation of glycerinated muscle: low-angle x-ray diffraction studies. *J. Mol. Biol.* **65**:331–354.
33. SATO, H., G. W. ELLIS, and S. INOUÉ. 1975. Microtubular origin of mitotic spindle form birefringence: demonstration of the applicability of Wiener's equation. *J. Cell Biol.* **67**:501–517.
34. SOLARO, J. R., D. C. PANG, and F. N. BRIGGS. 1971. The purification of cardiac myofibrils with triton X-100. *Biochim. Biophys. Acta.* **245**:259–268.
35. SPUDICH, J. A., H. E. HUXLEY, and J. T. FINCH. 1972. Regulation of skeletal muscle contraction. II. Structural studies of the interaction of the tropomyosin-troponin complex with actin. *J. Mol. Biol.* **72**:619–628.
36. TAYLOR, D. L. 1973. Exploration of molecular organization in cells using polarized light. Ph.D. Thesis. State University of New York at Albany. Albany, N. Y.
37. TAYLOR, D. L. 1975. Birefringence changes of vertebrate striated muscle. *J. Supramol. Struct.* **3**:181–191.
38. TAYLOR, D. L., R. D. ALLEN, and E. P. BENDITT. 1975. Determination of the polarization optical properties of the amyloid congo red complex by phase modulation microspectrophotometry. *J. Histochem. Cytochem.* **22**:1105–1112.
39. VON MURALT, A. 1933. Über das Verhalten der Doppelbrechung des quergestreiften Muskels während der Kontraction. *Pfuegers Archiv Gesamte Physiol. Menschen Tiere.* **230**:299–308.
40. WHITE, D. C. S. 1970. Rigor contraction and the effect of various phosphate compounds on glycerinated insect flight and vertebrate muscle. *J. Physiol.* **208**:583–604.
41. WIENER, O. 1912. Die theorie des Mischkörpers für der Fall der stationären Strömung—I. *Die Mittelwertzätze Math. Phys. Kl.* **32**:509–604.